Physica Scripta

INCLUSIVE PUBLISHING
TRUSTED SCIENCE

PAPER • OPEN ACCESS

Effects of boron doping in InSe single crystals on optical limiting performance in the near-infrared region

To cite this article: Anıl Doğan *et al* 2024 *Phys. Scr.* **99** 045505

View the article online for updates and enhancements.

You may also like

- Optical determination of layered-materials InSe thickness via RGB contrast method and regression analysis
Yi-Ying Lu, Hsiao-Ching Yu, You-Xin Wang et al.
- Direct Z-scheme photocatalytic overall water splitting on 2D CdS/InSe heterostructures
Yingcai Fan, Bo Yang, Xiaohan Song et al.
- Super deformability and thermoelectricity of bulk -InSe single crystals
Bin Zhang, , Hong Wu et al.

This content was downloaded from IP address 80.251.45.167 on 17/03/2024 at 22:00

Physica Scripta

PAPER

Effects of boron doping in InSe single crystals on optical limiting performance in the near-infrared region

Anıl Doğan[1], **Yasemin Pepe**[1], **Meliha Yağmur Bilgili**[1,2], **Ahmet Karatay**[1,*], **Hüseyin Ertap**[3,*], **Mevlüt Karabulut**[4] **and Ayhan Elmali**[1]

[1] Department of Engineering Physics, Faculty of Engineering, Ankara University, 06100, Ankara, Turkey
[2] Department of Command Control and Defence Technologies, HAVELSAN, 06510, Ankara, Turkey
[3] Department of Physics, Faculty of Science and Letter, Kafkas University, 36100, Kars, Turkey
[4] Department of Physics, Gebze Technical University, 41400, Gebze/Kocaeli, Turkey
[*] Authors to whom any correspondence should be addressed.

E-mail: akaratay@eng.ankara.edu.tr **and** huseyinertap@kafkas.edu.tr

Keywords: two photon absorption, open aperture Z-scan, InSe single crystal, optical limiting

OPEN ACCESS

RECEIVED
23 June 2023

REVISED
27 December 2023

ACCEPTED FOR PUBLICATION
23 January 2024

PUBLISHED
6 March 2024

Original content from this work may be used under the terms of the Creative Commons Attribution 4.0 licence.

Any further distribution of this work must maintain attribution to the author(s) and the title of the work, journal citation and DOI.

Abstract

Identification of photonic materials with high infrared transmittance and high nonlinear optical coefficients is one of the main emphases in material science as a result of the rapid advancement in infrared photonics. In this study, undoped and B (boron) -doped InSe single crystals were grown by using the modified vertical Bridgman method, and their nonlinear optical properties were investigated to reveal their usability as an optical limiter in the near-infrared region. The decreasing band gap energies and increasing defect states were determined with increasing B concentration in InSe single crystals. The effect of the B concentration on the nonlinear absorption (NA) and optical limiting properties of the InSe single crystals was investigated via open aperture (OA) Z-scan experiments under ultrafast laser excitation at 1200 nm wavelength with 100 femtosecond pulse duration. Two-photon absorption (TPA) was the dominant NA mechanism at 1200 nm excitation wavelength in the femtosecond domain. The results revealed that the NA became stronger with increasing input intensity and increasing amount of B dopant atoms in the InSe single crystal. The observed enhanced NA can be attributed to two possible events (i) increasing input intensity induced more excited electrons which led to more contribution to NA through TPA and (ii) increasing B dopant atoms in InSe single crystal induced more defect states. The NA may be more enhanced with the contribution of these defect states related NA mechanisms. The high transparency and strong NA behavior at the near-infrared region make these single crystals exceptional potential candidates for developing various optoelectronics and filters at the near-infrared spectral region.

1. Introduction

Indium Selenide (InSe), a complex layered (Se-In-In-Se) semiconductor compound, is an essential member of III–VI group compounds. In the literature, there are many studies on the determination of linear and nonlinear optical properties of InSe materials doped with various elements such as Ho, Dy, Er, Al, and Ag [1–5]. Three forms of InSe (thin film, nanosheet, and single crystal) have been generally investigated for optoelectronic applications such as phase change memory, solar cells, diode, and photodetector [6–9].

Nonlinear optical responses of materials provide significant benefits for various applications such as Q-switched fiber laser, optical limiting, and mode-locking [10–12]. In the nonlinear optical experiments, InSe materials are excited with beams in the infrared region due to their narrow band gap energies (~1.3 eV) and exhibit two types of nonlinear response: (i) Nonlinear absorption (NA) which includes two-photon absorption (TPA), multi-photon absorption (MPA), and free-carrier absorption (FCA), and (ii) saturable absorption (SA) [1, 13, 14]. The increase in the nonlinear absorption coefficient with increasing optical intensity causes NA. This behavior is an important property for materials to be used as an optical limiter. An optical limiter (OL) is used to

© 2024 The Author(s). Published by IOP Publishing Ltd

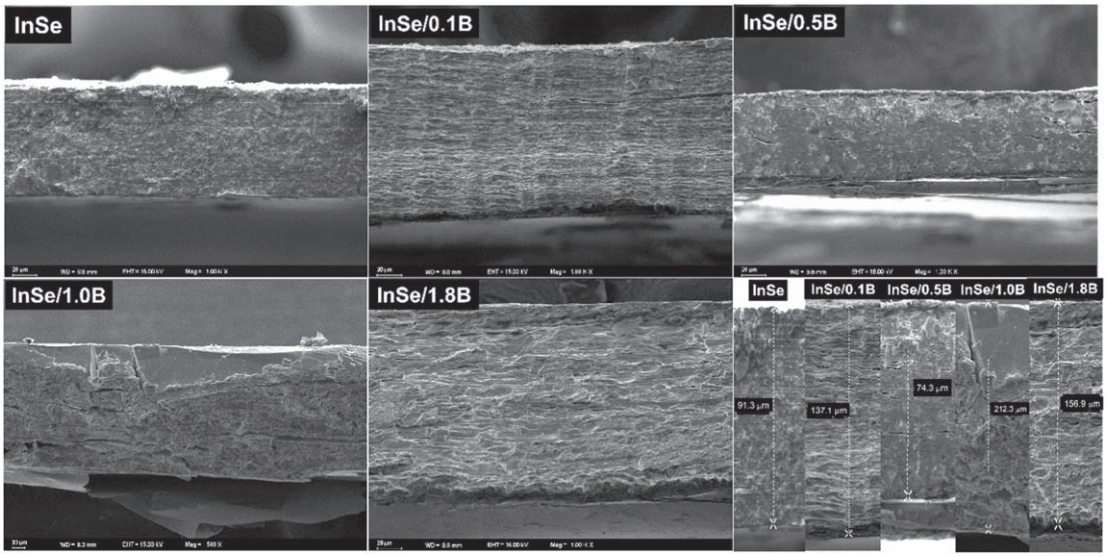


Figure 1. SEM images of undoped and B-doped InSe single crystals.

protect human eyes and optical detectors from irreversible damage by highly intense laser pulses from visible to infrared range. The optical limiting property of a material is based on nonlinear optical phenomena such as NA, nonlinear scattering, nonlinear refraction, and TPA [15–21]. An optical limiter allows light to pass through when the intensity of light is weak. If the intensity of light is sufficiently high, the optical limiter begins to absorb the light and causes a decrease in transmission. Considering the human eyes, a few μJ energy of light can lead to irreversible damage [22]. Therefore, the limiting threshold of an optical limiter material should be as low as possible for protecting human eyes. With the development of infrared high-intensity lasers, especially at short wavelength infrared (SWIR) band, optical limiting (OPL) devices are in demand for many application fields such as biomedicine, remote sensing, eye-safe LIDAR (Light Detection And Ranging) systems, active imaging, telemetry, autonomous vehicles guiding systems, and molecular spectroscopy [23–27]. Therefore, infrared OPL devices are quite important for various technologies, and demands for them are increasing day by day.

Linear optical and electrocatalyst features of B-doped InSe materials were investigated as a single crystal and monolayer [28, 29]. However, although there is much research on the nonlinear optical properties of InSe materials [1, 4, 13, 14, 30–35], there are no studies that make an effort to design InSe single crystal as an effective optical limiter in near-infrared (IR) region. This study reveals the effective composition of the B-doped InSe single crystal as an efficient optical limiter in near IR region. In this way, it was aimed to tune the band gap with B atoms to support TPA to facilitate their use in the near IR region. The open aperture (OA) Z-scan experiments were performed at 1200 nm with a femtosecond pulsed laser with increasing input intensity to examine the behavior of the optical limiting behavior in the near IR region.

2. Experimental processes

2.1. Growth of undoped and B-doped InSe single crystals

Undoped and different amounts (0.1%, 0.5%, 1.0%, and 1.8%) of B-doped InSe single crystals were grown by using the modified vertical Bridgman method. To grow undoped and B-doped InSe single crystals, a stoichiometric mixture of high purity In (99.9999%), Se (99.999%), and B (99.7%) in evacuated quartz ampoules (10^{-4} Torr) whose inner walls were coated with carbon. Undoped and B-doped InSe compounds were synthesized at 800 °C for 48 h. After the synthesis, the quartz ampoules firstly were positioned vertically in the modified Bridgman furnace. The growth temperature of undoped and B-doped InSe single crsytals is 660 °C. The details are given elsewhere [28, 36–38]. The prepared undoped and B-doped InSe single crystal ingots had no cracks and voids on the surface. No polishing and cleaning were made for all samples due to their perfect mirror-like surfaces. Ingots were cleaved perpendicular to the c-axis using a razor blade. The dimensions of all samples prepared from the bulk ingots for the nonlinear optical measurements were approximately 1 cm × 1 cm. Doping concentration of InSe single crystals are atomic percentage. Also, the elemental compositions of the single crystals were determined by Inductively Coupled Plasma (ICP) spectroscopy. InSe single crystals are labeled InSe for undoped and InSe/0.1B, InSe/0.5B, InSe/1.0B, and InSe/1.8B for 0.1%, 0.5%, 1.0%, 1.8% B-doped samples, respectively.

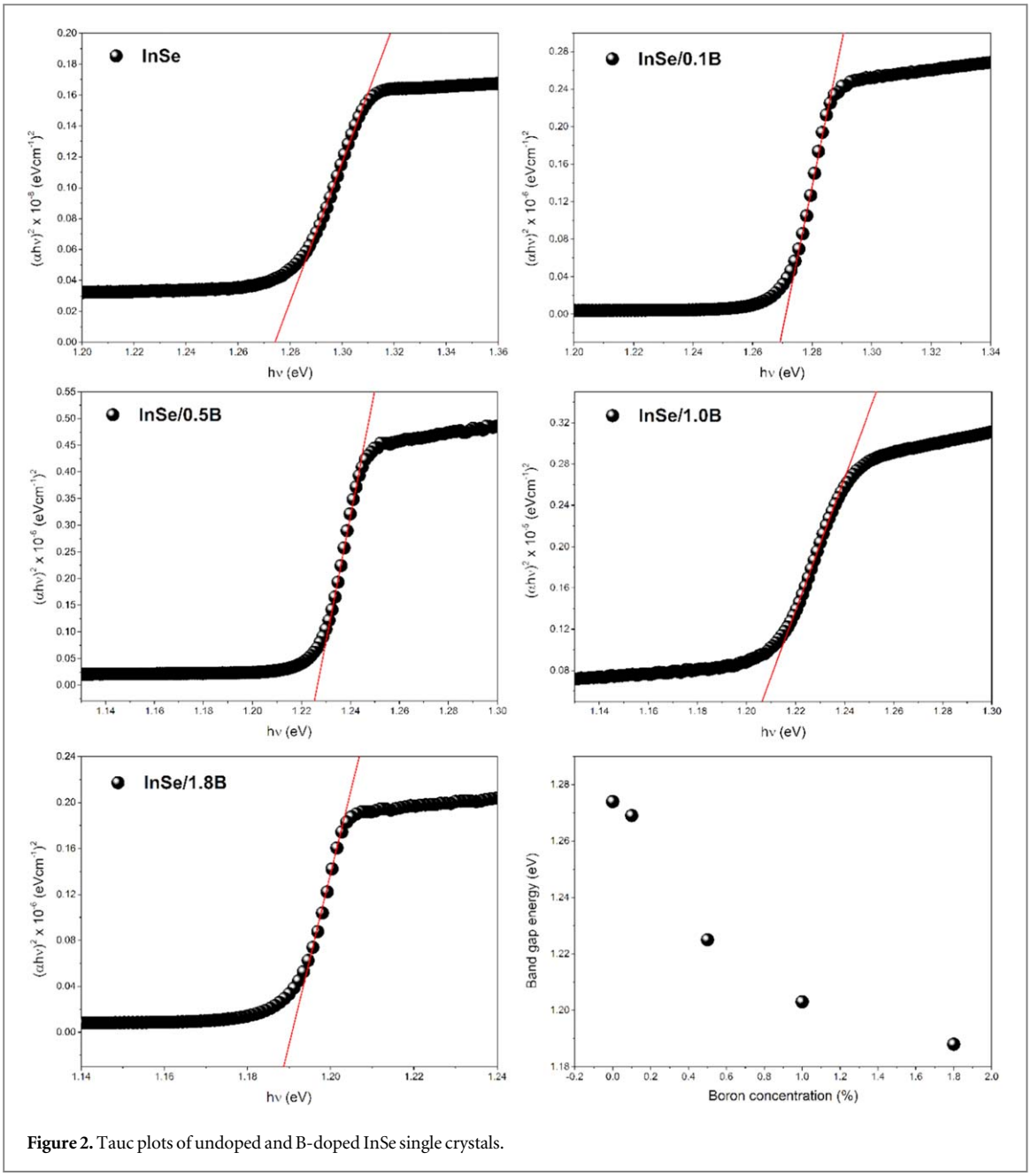


Figure 2. Tauc plots of undoped and B-doped InSe single crystals.

2.2. Characterization methods

The structure of undoped and B-doped InSe single crystals was previously studied by XRD [37]. The thicknesses of the undoped and B-doped InSe single crystals were determined by scanning electron microscope (ZEISS EVO 40). The absorption spectra of the crystal materials were obtained through a Shimadzu UV- 1800 model UV/VIS absorption spectrophotometer. The nonlinear optical absorption experiments were performed via the open aperture (OA) Z-scan technique by using an ultrafast laser at 1200 nm wavelength with 100 femtosecond (fs) pulse duration and 1 kHz frequency. The crystals were fixed on a computer-controlled translational stage and the laser beam focused via a 20 cm convex lens. The radius of the beam was measured to be 40 μm at the focal point. The transmitted beams from the samples were measured by silicon detector and boxcar average.

3. Results and discussions

3.1. Structural and linear optical properties

The XRD pattern of the studied single crystals was reported in [37]. It was reported that the crystallinity of the InSe single crystal decreased with the increase of the B doping concentration and this result was attributed to the increased structural defects. The strain values were calculated to be 4.766 for InSe, 4.818 for InSe/0.1B, 4.931 for InSe/0.5B, and 5.947 for InSe/1.8B crystals. A decrease in d values were also observed with B addition [34].

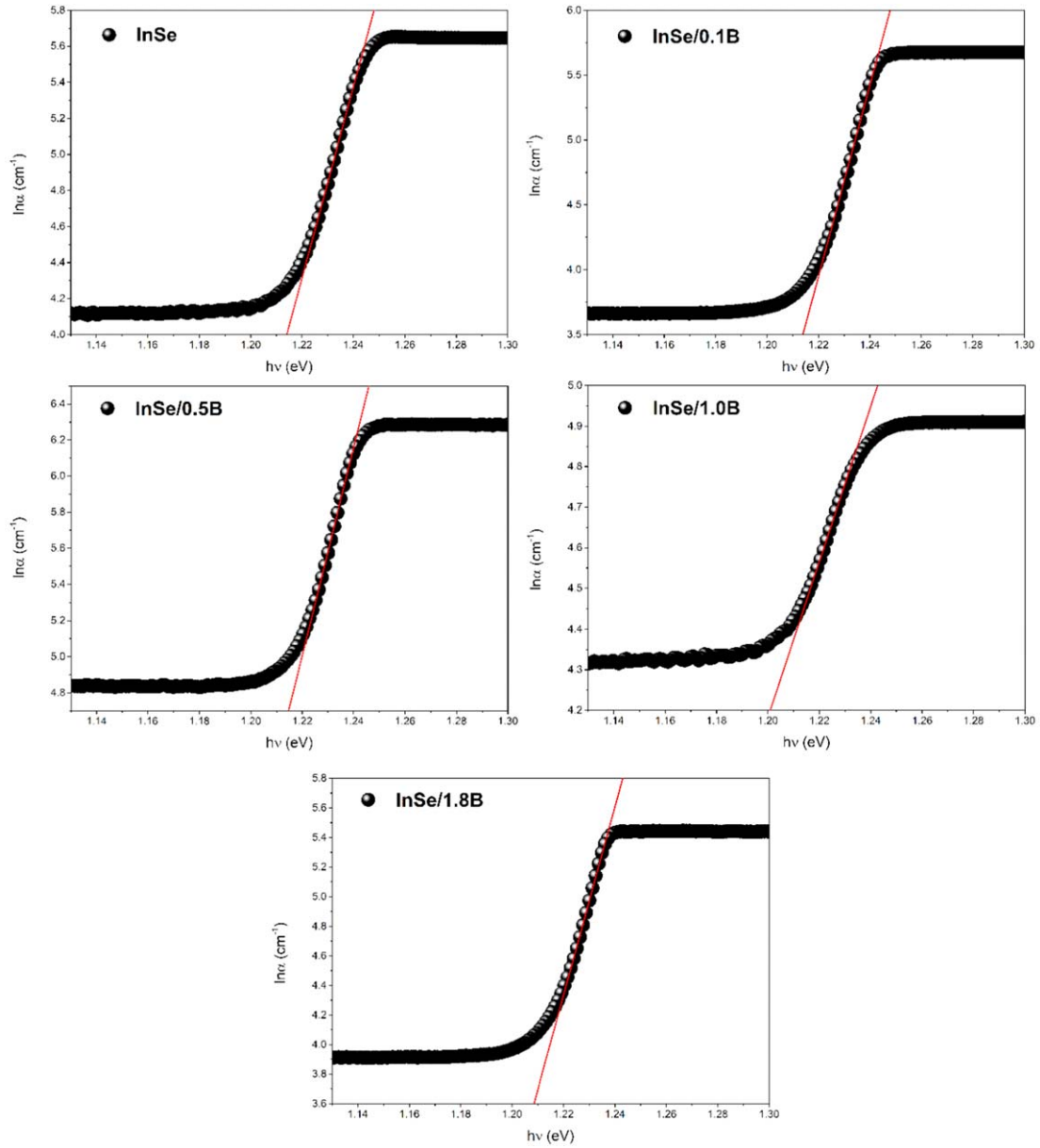


Figure 3. ln α versus $h\nu$ plots of undoped and B-doped InSe single crystals.

Table 1. Comparison of the band gap energies of B, Ho, Dy, Al, and Ag-doped InSe materials.

Materials	E_g (eV)	References
InSe single crystal	1.274	
InSe/0.1B single crystal	1.269	Present
InSe/0.5B single crystal	1.225	work
InSe/1.0B single crystal	1.203	
InSe/1.8B single crystal	1.188	
InSe: Ho (0.005%)	1.228	[1]
InSe: Ho (0.05%)	1.235	
n-InSe: Dy	1.263	[2]
Al-doped InSe (1.5 W)	2.44	
Al-doped InSe (2.0 W)	2.32	[4]
Al-doped InSe (2.5 W)	2.25	
InSe: Ag	1.302	[5]

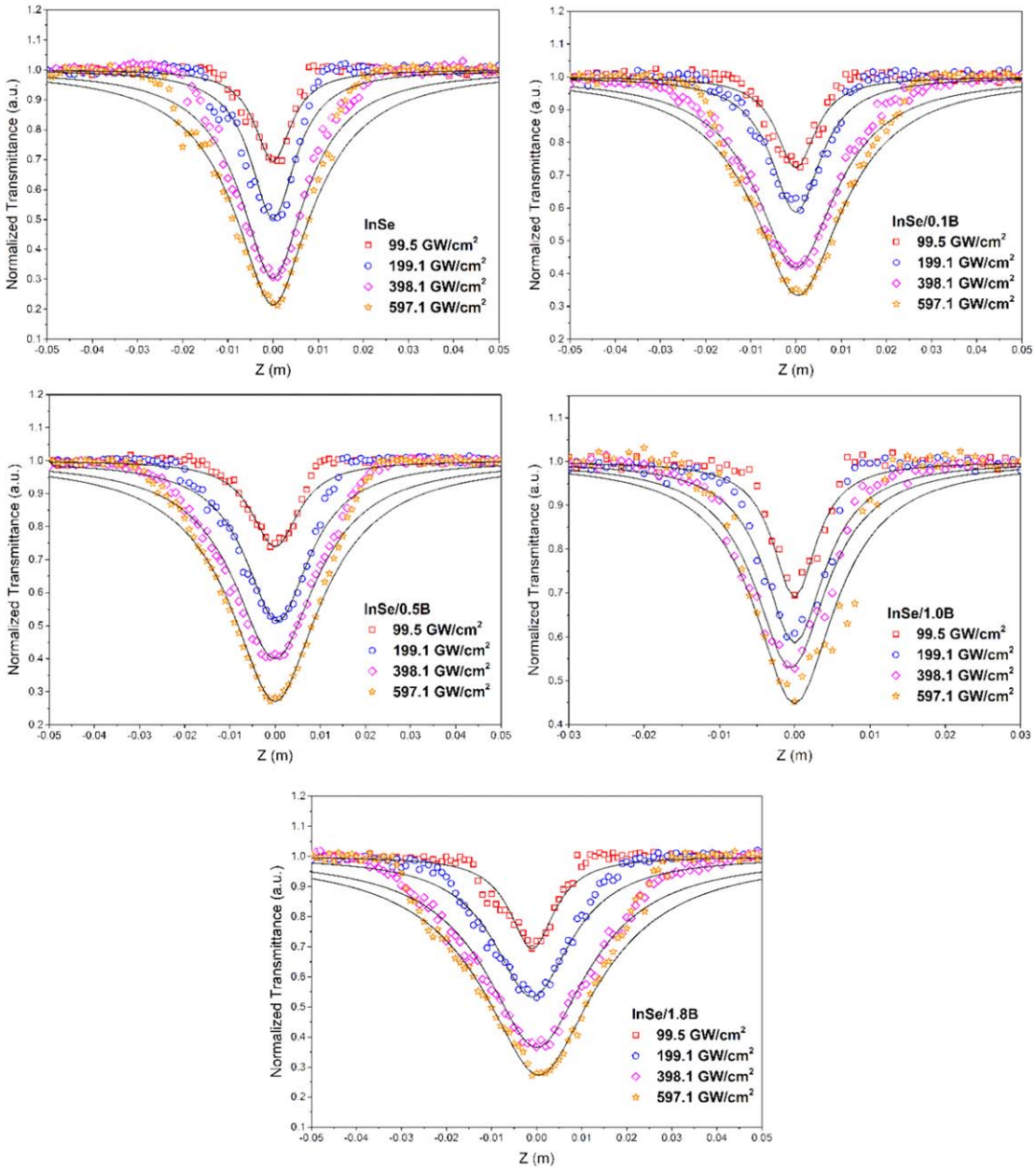


Figure 4. Open aperture Z-scan traces of B-doped and undoped InSe single crystals at various input intensities.

Similar change in the band gap with the addition of B in InSe, as observed in other layered crystal [39]. The thicknesses of the InSe single crystals presented in figure 1 were determined as 91.3, 137.1, 74.32, 207.0, and 152.8 μm for InSe, InSe/0.1B, InSe/0.5B, InSe/1.0B, and InSe/1.8B, respectively.

Nonlinear absorption mechanisms are closely related to the band gap energy and the defect density of the materials. Band gap energies of InSe, InSe/0.1B, InSe/0.5B, InSe/1.0B, and InSe/1.8B single crystals calculated from Tauc plots (seen in figure 2) as given in [38], and its values are 1.274, 1.269, 1.225, 1.203 and 1.188 eV, respectively. Band gap energies of InSe single crystals decrease with increasing B concentration relative to the band gap energy of undoped InSe single crystals. In our previous papers, a similar decrease in band gap energy with B addition was observed from the CPM and photoluminescence measurements [28, 40]. In general, band gap energies of undoped and different elements doped InSe single crystal is reported to be in the 1.2–1.3 eV interval [2, 28, 40–44]. B-doped InSe materials have relatively lower band gap energies at room temperature compared to InSe materials doped with other elements such as Ho, Dy, Al, and Ag, as seen in table 1.

The band gap energies given in the present study are consistent with theliterature. The shifting of band gap energies to lower values in the B-doped InSe single crystals is obviously related to the B addition. However, we should note that there are several mechanisms for the incorporation of boron atoms into the lattice: they may substitute with greater size In atoms ($r_{In} = 0.94$ Å, and $r_B = 0.41$ Å), intercalate between the layers or occupy

Table 2. I_0 and β values of InSe single crystals from the Z-scan curve fit with different laser intensities.

Materials	I_0 (GW/cm^2)	$\beta \times 10^{-10}$ (cm/W)
InSe	99.5	0.58
	199.1	1.14
	398.1	1.41
	597.1	1.58
InSe/0.1B	99.5	5.49
	199.1	5.75
	398.1	7.24
	597.1	7.49
InSe/0.5B	99.5	11.4
	199.1	13.6
	398.1	16.5
	597.1	20.8
InSe/1.0B	99.5	33.8
	199.1	37.1
	398.1	38.8
	597.1	40.2
InSe/1.8B	99.5	63.0
	199.1	87.0
	398.1	114.8
	597.1	117.5

Table 3. NA coefficients of InSe single crystals dependent on B concentration at 99.5 GW/cm^2 laser intensity.

Materials	$h\nu/E_g$	$\beta \times 10^{-10}$ (cm/W)
InSe	0.81	0.58
InSe/0.1B	0.82	5.49
InSe/0.5B	0.84	11.4
InSe/1.0B	0.86	33.8
InSe/1.8B	0.87	63.0

interstitial positions which may have different effects on lattice parameters and unit cell volume. Similar variations in lattice parameters were also observe in boron doped GaSe single crystals [45].

Figure 3 shows ln α - $h\nu$ plots of undoped and B-doped InSe single crystals. The distribution of the defect states localized inside the band gap of the crystals can be determined by the following equation [46],

$$\alpha = \alpha_0 \exp\left(h\nu/E_U\right) \tag{1}$$

Where α is the absorption coefficient, α_0 is a constant, and E_U is the Urbach energy. The distribution of the defect states inside the band gap is proportional to the Urbach energy. The Urbach energies of the crystals can be calculated from the inverse slope of the linear regions of the ln α-$h\nu$ curves. The Urbach energy of the undoped single crystal was found to be 0.013 eV and it increased to 0.054 eV with increasing the B concentration in InSe single crystal which follows the results given in [40]. The Urbach energy values represent that the defect states are distributed below the conduction band of the crystals.

3.2. Nonlinear optical properties

The nonlinear absorption behaviors of the undoped and B-doped InSe single crystals from the fits of OA Z-scan measurements under 1200 nm wavelength excitations at 100 fs pulse duration are given in figure 4. As seen in figure 4, the transmittance of all crystals decreased depending on increasing of the optical intensity, which is called NA. The optical nonlinearity can be defined in the following equation [45],

$$\alpha(I) = \alpha_0 + \beta I \tag{2}$$

where α_0 and β are linear absorption and TPA coefficients, respectively. The transmittance can be given by the equation (4),

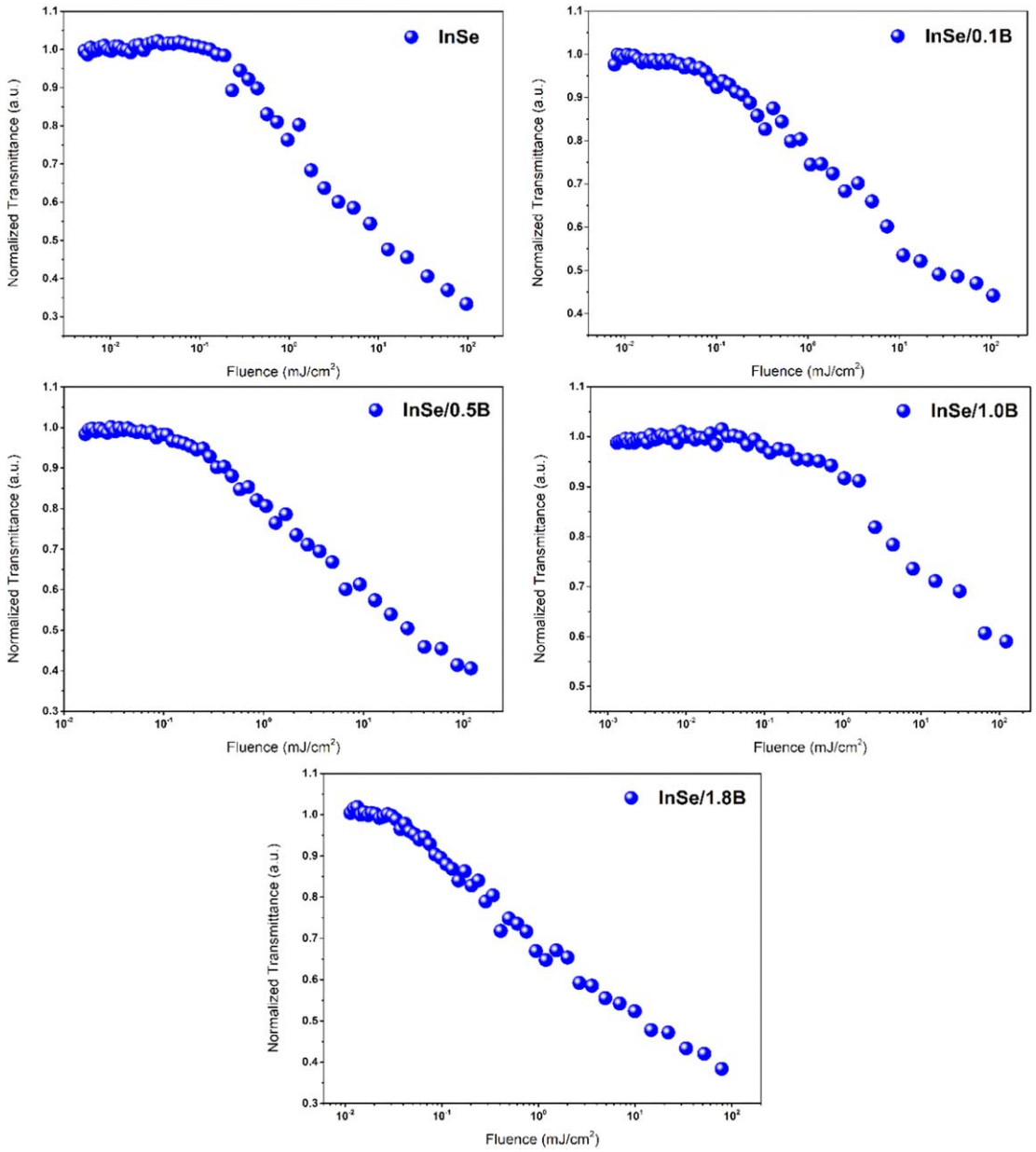


Figure 5. Optical limiting curves of InSe single crystals.

$$T(z, S=1) = \frac{1}{\sqrt{\pi}\rho_0(z, 0)} \int_{-\infty}^{\infty} \ln\left[1 + \rho_0(z, 0)e^{-\tau^2}\right] d\tau \tag{3}$$

where $\rho_0(z, 0) = \beta I_0 L_{eff}/(1 + z^2/z_0^2)$, z is the position of the material and $z = 0$ at he focus, $z_0 = k\omega_0^2/2$ is the Rayleigh range, ω_0 is the beam waist at focus, I_0 is the intensity of laser beam at the focus, and L_{eff} is the effective thickness of the material and given as $L_{eff} = [1 - e^{-\alpha_0 L}]/\alpha_0$, L is the thickness of the material.

The TPA coefficient values of all crystals at different input intensities are given in table 2. It is seen that the β values increased with increasing intensity of the laser beam for each crystal. The increasing input intensity induces more excited electrons which leads to more contribution to NA through TPA. Yüksek *et al* investigated the nonlinear optical properties of Ho-doped InSe single crystals, and they observed that the Ho-doped InSe single crystals exhibit SA at low input intensities at 1064 nm with 65 ps pulse duration. It is due to the lifetime of the defect states is shorter than the pulse duration and defect states can fill at low intensities [1]. X Yan *et al* observed reverse saturable absorption (RSA) in Al-doped InSe thin films from the results of transient absorption experiments. It is attributed that Al nanoparticles trap the excited electrons and inhibit the recombination process. Therefore, Al doping provides stronger excited state absorption (ESA) [4]. The B-doped InSe single crystals have higher β values than that of undoped InSe single crystals as seen in table 2. As reported in [37], the doping of B atoms in InSe single crystal caused to decrease in the crystallite size and increasing defect states. As reported in our previous studies [14, 47, 48], the reaction of more localized defect states with doping of the

Table 4. Optical limiting thresholds of undoped and B-doped InSe single crystals and different nonlinear optical materials in the literature with excitation wavelengths and pulse durations.

Materials	λ_{exc} (nm)	Pulse duration	Limiting thresholds	References
InSe single crystal	1200	100 fs	0.106 mJ/cm^2	
InSe/0.1B single crystal			0.076 mJ/cm^2	
InSe/0.5B single crystal			0.065 mJ/cm^2	
InSe/1.0B single crystal			0.049 mJ/cm^2	Present work
InSe/1.8B single crystal			0.027 mJ/cm^2	
Al-doped InSe (2.5 W)	532–1064	190 fs	11–19 mJ/cm^2	
Al-doped InSe (2.0 W)			13–25 mJ/cm^2	[4]
Al-doped InSe (1.5 W)			21–45 mJ/cm^2	
Pure Bi_2WO_6	532	9 ns	9.88×10^{12} W m^{-2}	
1% Zn / Bi_2WO_6			8.78×10^{12} W m^{-2}	[52]
3% Zn / Bi_2WO_6			7.88×10^{12} W m^{-2}	
5% Zn / Bi_2WO_6			6.22×10^{12} W m^{-2}	
7% Zn / Bi_2WO_6			13.7×10^{12} W m^{-2}	
NBiBEu0 Glass	1000	150 fs	0.390 J m^{-2}	
NBiBEu0.5 Glass			0.254 J m^{-2}	[53]
NBiBEu1 Glass			0.143 J m^{-2}	
NBiBEu1.5 Glass			0.084 J m^{-2}	
NBiBEu2 Glass			0.042 J m^{-2}	
$PbMoO_4$ single crystal	532	4 ns	4.91 mJ/cm^2	[54]
2D-CdSe nanostructure	800	56 fs	1.9 mJ/cm^2	[55]
$Bi_{12}TiO_{20}$ single crystal	532	4 ns	6.62 mJ/cm^2	[56]
	1064		5.45 mJ/cm^2	
$Bi_{12}SiO_{20}$ single crystal	532	4 ns	0.34 mJ/cm^2	[57]
	1064		0.68 mJ/cm^2	
DMMC single crystal	800	150 fs	5.6 mJ/cm^2	[58]
LPPF single crystal	794	150 fs	2.45 mJ/cm^2	[59]

crystal led to enhanced NA behavior. The energy of the excitation photons (1200 nm) was 1.03 eV which is not enough to excite the localized defect states inside the band gap. On the other hand, these localized defect states could be distributed to the larger energy region considering to their Urbach energies. In this case, the excess localized defect states created by increasing B concentration can contribute to NA through one-photon absorption. In our previous study, we pointed out that the TPA performance of the material was related to the ratio between the input energy and band gap energy, and it increased with the increasing the ratio of $h\nu/E_g$ [49, 50]. The changes in the β values of the crystals at the same input intensity with the ratios of $h\nu/E_g$ are listed in table 3. These results reveal that the TPA is the dominant NA mechanism among other NA mechanisms in the femtosecond time domain at 1200 nm excitation wavelength for these crystals.

3.3. Optical limiting properties

The optical limiting features of undoped and B-doped InSe single crystals were investigated under the excitations of 100 fs laser pulse at 1200 nm wavelength. The normalized transmittances of the crystals were plotted against laser fluence and given in figure 5. Fluence was calculated using the following expression depending on the distance [51],

$$I(z) = \frac{E}{\pi\omega^2(z)t} = \frac{Q}{t} \tag{4}$$

where Q is the fluence which is the energy per beam area and t is the pulse duration, E is the energy of incident beam per pulse, $\omega(z)$ is the beam waist which depends on the distance. To determine the beam waist, the relations for the Gaussian beam are given in equations (8) and (9),

$$\omega^2(z) = \omega_0^2\left(1 + \frac{z^2}{z_R^2}\right) \tag{5}$$

$$z_R = \frac{\pi\omega_0^2}{\lambda} \tag{6}$$

where z_R is the Rayleigh distance, λ is the wavelength of the incident beam, and ω_0 is the beam waist at focus.

As seen in figure 5, the transmittance of the crystals begins to decrease sharply when the fluence of the incident beam reaches a threshold value for the crystals. For this reason, the undoped and B-doped InSe single crystals behave as optical limiters at high intensities which correspond to fluence values higher than the limiting

thresholds. The optical limiting threshold values of the crystals were found in the range of 0.106–0.027 mJ/cm^2 at 398.1 GW/cm^2 laser intensity. The lower optical limiting threshold was found as 0.027 mJ/cm^2 for higher B-doped InSe single crystal. The decrease in the optical limiting thresholds with increasing B concentration can be attributed to the stronger NA behavior. Therefore, B doping in the InSe single crystals provides more effective results for near-infrared optical limiting applications than the undoped InSe single crystal. Additionally, the comparison of the limiting thresholds of the undoped and B-doped InSe single crystals and similar materials in the literature at different excitation wavelengths and pulse durations is listed in table 4. Further, 1.8% B-doped InSe single crystal has the lowest limiting threshold for near-infrared excitations compared with the other optical limiting materials given in the table. Consequently, B-doped InSe single crystals are quite useful nonlinear optical materials for near-infrared optical limiting applications.

4. Conclusion

Most commercially available lasers operate in the near-infrared region, so it is crucial to study optical nonlinearities in this spectral range as well as to achieve good optical performance at non-resonant wavelengths to successfully demonstrate the materials' potential for use in nonlinear optical devices. In addition, materials with large TPA capability are highly useful for optical limiting. For that reason, B atoms were doped in different concentrations to undoped InSe single crystal to tune band gap energies, which in turn increased TPA at 1200 nm excitation wavelength. The band gap energies decreased from 1.27 to 1.18 eV with increasing B concentration via the localized defect states just below the conduction band. On the other hand, more localized defect states were created by increasing doping of B in InSe single crystal. The results of the OA Z-scan experiments indicated that the NA behaviors of the crystals tend to increase with increasing input intensity. Besides, the increasing B atoms in the InSe single crystal led to increasing TPA contribution to NA. The higher NA coefficient was found for higher B-doped InSe single crystal as 11.75×10^{-9} m W^{-1} at 597.1 GW/cm^2 input intensity. Further, the B effect on the optical limiting behavior of the InSe single crystals was also investigated. The lowest optical limiting threshold was found as 0.027 mJ/cm^2 for the highest B concentration in InSe single crystal. Considering the higher transmittance and stronger NA behavior, undoped and B-doped InSe single crystals can be used as an effective optical limiter in the near-infrared region.

Data availability statement

All data that support the findings of this study are included within the article (and any supplementary files).

ORCID iDs

Yasemin Pepe https://orcid.org/0000-0002-5384-2039
Ahmet Karatay https://orcid.org/0000-0001-9373-801X
Hüseyin Ertap https://orcid.org/0000-0003-3896-6188

References

[1] Yuksek M *et al* 2014 Nonlinear and saturable absorption characteristics of Ho doped InSe crystals *Opt. Commun.* **310** 100–3
[2] Gurbulak B 1999 Growth and optical properties of Dy doped and undoped n-type InSe single crystal *Solid State Commun.* **109** 665–9
[3] Abay B *et al* 1998 Urbach-martienssen tails in Er-doped and undoped n-type InSe *Physica B-Condensed Matter* **254** 148–55
[4] Yan X Y *et al* 2020 Ultrafast broadband reverse saturation absorption in Al-doped InSe thin films for optical limiting at visible/near-infrared *Opt. Mater.* **108** 110171
[5] Gurbulak B *et al* 2014 Structural characterizations and optical properties of InSe and InSe:Ag semiconductors grown by bridgman/stockbarger technique *Physica E-Low-Dimensional Systems & Nanostructures* **64** 106–11
[6] Lee H, Kang D H and Tran L 2005 Indium selenide (In_2Se_3) thin film for phase-change memory *Materials Science and Engineering B-Solid State Materials for Advanced Technology* **119** 196–201
[7] Mondal B K *et al* 2021 Effect of CdS and In_3Se_4 BSF layers on the photovoltaic performance of PEDOT:PSS/n-Si solar cells: simulation based on experimental *data Superlattices Microstruct.* **152** 106853
[8] Matheswaran P, Sathyamoorthy R and Asokan K 2012 Schottky nature of InSe/Cu thin film diode prepared by sequential thermal evaporation *Electron. Mater. Lett.* **8** 621–6
[9] Li Z J *et al* 2018 High-Performance photo-electrochemical photodetector based on liquid-exfoliated few-layered inse nanosheets with enhanced stability *Adv. Funct. Mater.* **28** 1705237
[10] Wang M *et al* 2014 Passively Q-switched Er-doped fiber laser using a semiconductor saturable absorber mirror *Optik* **125** 2154–6
[11] Yuan C G *et al* 2022 Nonlinear absorption, refraction and optical limiting properties of CsPbBr3 perovskite quantum dot organic glass *Opt. Mater.* **134** 113090
[12] Zhang H *et al* 2010 Compact graphene mode-locked wavelength-tunable erbium-doped fiber lasers: from all anomalous dispersion to all normal dispersion *Laser Phys. Lett.* **7** 591–6

[13] Pan H *et al* 2019 Broadband nonlinear optical response of InSe nanosheets for the pulse generation from 1 to 2 mu m *ACS Appl. Mater. Interfaces* **11** 48281–9
[14] Yuksek M *et al* 2010 Nonlinear and saturable absorption characteristics of amorphous InSe thin films *J. Appl. Phys.* **107** 033115
[15] Mansour K, Soileau M J and Vanstryland E W 1992 Nonlinear optical-properties of carbon-black suspensions (Ink) *Journal of the Optical Society of America B-Optical Physics* **9** 1100–9
[16] Leite R C C, Porto S P S and Damen T C 1967 The thermal lens effect as a power-limiting device *Applied Physics Letter* **10** 100–1
[17] Four M *et al* 2011 A novel ruthenium(II) complex for two-photon absorption-based optical power limiting in the near-IR range *Phys. Chem. Chem. Phys.* **13** 17304–12
[18] Cha M *et al* 1995 Enhanced nonlinear absorption and optical limiting in semiconducting polymer methanofullerene charge transfer films *Appl. Phys. Lett.* **67** 3850–2
[19] Isık P *et al* 2013 The effect of film thickness, Se/S ratio and annealing temperature on the nonlinear and saturable absorption behaviors in amorphous $GaSe_xS_{1-x}$ ($0 \leqslant x \leqslant 1$) thin films *Opt. Commun.* **288** 107–13
[20] Ünlü B A *et al* 2022 Defect assisted nonlinear absorption and optical limiting in amorphous $TlGaS_{2\,(1-x)}\,Se_{2\,(x)}$($0 \leqslant x \leqslant 1$) thin films *J. Lumin.* **241** 118540
[21] Ünlü B A *et al* 2020 The effect of Ga/In ratio and annealing temperature on the nonlinear absorption behaviors in amorphous $TlGa_xIn_{(1-x)}S_2$ ($0 \leqslant x \leqslant 1$) chalcogenide thin films *Opt. Laser Technol.* **128** 106230
[22] Miles P A 1994 Bottleneck optical limiters: the optimal use of excited-state absorption *Appl. Opt.* **33** 6965–79
[23] Waynant R W, Ilev I K and Gannot I 2001 Mid-infrared laser applications in medicine and biology *Philosophical Transactions of the Royal Society of London Series a-Mathematical Physical and Engineering Sciences* **359** 635–44
[24] Walsh B M, Lee H R and Barnes N P 2016 Mid infrared lasers for remote sensing applications *J. Lumin.* **169** 400–5
[25] Pascal S *et al* 2019 Unraveling the two-photon and excited-state absorptions of Aza-BODIPY dyes for optical power limiting in the SWIR band *J. Phys. Chem. C* **123** 23661–73
[26] David S *et al* 2020 High-Performance optical power limiting filters at telecommunication wavelengths: when Aza-BODIPY Dyes bond to sol-gel materials *J. Phys. Chem. C* **124** 24344–50
[27] Vainio M and Karhu J 2017 Fully stabilized mid-infrared frequency comb for high-precision molecular spectroscopy *Opt. Express* **25** 4190–200
[28] Ertap H, Bacioglu A and Karabulut M 2015 Photoluminescence properties of boron doped InSe single crystals *J. Lumin.* **167** 227–32
[29] Ma B Y *et al* 2019 Boron-doped InSe monolayer as a promising electrocatalyst for nitrogen reduction into ammonia at ambient conditions *Appl. Surf. Sci.* **495** 143463
[30] Yuksek M 2012 Nonlinear refraction effects of amorphous semiconductor InSe thin films according to film thicknesses and/or pulse durations *Opt. Commun.* **285** 5472–4
[31] Mondal B K, Rahman M F and Hossain J 2022 Unraveling the nonlinear optical behaviors of indium selenide thin films prepared by spin coating method *Results in Physics* **39** 105701
[32] Shu Y Q *et al* 2022 2D BP/InSe Heterostructures as a nonlinear optical material for ultrafast photonics *Nanomaterials* **12** 1809
[33] Chen C D *et al* 2022 Microscopic optical nonlinearities and transient carrier dynamics in indium selenide nanosheet *Opt. Express* **30** 17967–79
[34] Yan X Y *et al* 2019 Morphological and nonlinear optical properties of Al:InSe thin films *Opt. Mater. Express* **9** 2955–63
[35] Yang W Q, Xu N N and Zhang H N 2018 Nonlinear absorption properties of indium selenide and its application for demonstrating pulsed Er-doped fiber laser *Laser Phys. Lett.* **15** 105101
[36] Ertap H *et al* 2011 Pool-Frenkel thermoelectric modulation of excition photoluminescence in GaSe crystals *J. Lumin.* **13** 1376–9
[37] Ertap H and Karabulut M 2019 Structural and electrical properties of boron doped InSe single crystals *Mater. Res. Express* **6** 035901
[38] Pepe Y *et al* 2022 The role of defects on the transition from saturable absorption to nonlinear absorption of Bi12GeO20 single crystal under increasing laser excitation *J. Lumin.* **251** 119170
[39] Abdinov A S *et al* 2004 Photoluminescence of rare-earth-doped InSe and GaSe single crystals *Inorg. Mater.* **40** 567–9
[40] Bacıoğlu A *et al* 2014 Sub-bandgap analysis of boron doped InSe single crystals by constant photocurrent method *Opt. Mater.* **37** 70–3
[41] Giulio M D *et al* 1983 Photovoltaic effect in gold-indium selenide schottky barriers *J. Appl. Phys.* **54** 5839–43
[42] Likforman A *et al* 1975 Crystal-Structure of Indium Monoselenide (Inse) *Acta Crystallographica Section B-Structural Science* **31** 1252–4
[43] Sreekumar R *et al* 2006 SHI induced single-phase InSe formation at lower annealing temperature *Nuclear Instruments & Methods in Physics Research Section B-Beam Interactions with Materials and Atoms* **244** 190–3
[44] Segura A *et al* 1983 Photoconductivity and photovoltaic effect in indium selenide *J. Appl. Phys.* **54** 876–88
[45] Karatay A *et al* 2016 Influence of boron concentration on nonlinear absorption and ultrafast dynamics in GaSe crystals *Opt. Mater.* **60** 74–80
[46] Unlu B A *et al* 2021 Enhancement of nonlinear absorption in defect controlled ZnO polycrystalline thin films by means of Co-doping *Physica Status Solidi B-Basic Solid State Physics* **258** 2000539
[47] Karatay A *et al* 2011 The nonlinear and saturable absorption characteristics of Ga0.90In0.10Se and Ga0.85In0.15Se semiconductor crystals and their amorphous thin films *J. Opt.* **13** 075203
[48] Kürüm U *et al* 2010 The effect of thickness and/or doping on the nonlinear and saturable absorption behaviors in amorphous GaSe thin films *J. Appl. Phys.* **108** 063102
[49] Karatay A 2019 Controlling of two photon absorption properties by altering composition ratio of GaSxSe1-x crystals *Opt. Laser Technol.* **111** 6–10
[50] Karatay A *et al* 2017 The effect of Se/Te ratio on transient absorption behavior and nonlinear absorption properties of $CuIn_{0.7}Ga_{0.3}(Se_{1-x}Te_x)_2$ ($0 \leqslant x \leqslant 1$) amorphous semiconductor thin films *Opt. Mater.* **73** 20–4
[51] Sreeja V G *et al* 2021 Effects of reduced graphene oxide on nonlinear absorption and optical limiting properties of spin coated aluminium doped zinc oxide thin films *Thin Solid Films* **722** 138580
[52] Shanthi S *et al* 2023 Influence of Zn^{2+} doping on the nonlinear optical limiting characteristics of Bi_2WO_6 nanostructures for optical device applications *Mater. Chem. Phys.* **306** 127980
[53] Jalluri T D P V *et al* 2021 Photoluminescence and nonlinear optical investigations on Eu_2O_3 doped sodium bismuth borate glasses for solid state lighting and near-infrared optical limiting applications *Infrared Phys. Technol.* **116** 103784
[54] Pepe Y *et al* 2022 Nonlinear optical absorption characteristics of $PbMoO_4$ single crystal for optical limiter applications *Opt. Mater.* **133** 112963
[55] Kushavah D *et al* 2021 Ultrafast and nonlinear optical properties of two-dimensional CdSe nanostructures prepared using MoS_2 nanosheets as template *Physica E-Low-Dimensional Systems & Nanostructures* **130** 114682

[56] Pepe Y et al 2023 Wavelength dependence of the nonlinear absorption performance and optical limiting in Bi12TiO20 single crystal J. Lumin. 253 119494
[57] Dogan A et al 2023 Excitation wavelength dependent nonlinear absorption mechanisms and optical limiting properties of Bi12SiO20 single crystal Opt. Mater. 140 113882
[58] Patil P S et al 2016 Crystalline perfection, third-order nonlinear optical properties and optical limiting studies of 3, 4-Dimethoxy-4 '-methoxychalcone single crystal. Opt. Laser Technol. 81 70–6
[59] Nagaradona S and Dhanakotti R B 2018 Spectral, nonlinear optical and optical limiting properties of L-phenylalanine L-phenylalaninium formate single crystal Spectrochimica Acta Part a-Molecular and Biomolecular Spectroscopy 203 147–57